Journal of the European Ceramic Society **16** (1996) 989–993

S0955-2219(96)00022-9
0955-2219/96/$9.50

Preparation of Micro-Coiled ZrC Fibres by Vapour Phase Metallizing of Micro-Coiled Carbon Fibres

S. Motojima,[a] H. Asano[a] & H. Iwanaga[b]

[a]Department of Applied Chemistry, Faculty of Engineering, Gifu University, Gifu 501-11, Japan
[b]Faculty of Liberal Arts, Nagasaki University, Nagasaki 852, Japan

(Received 26 June 1995; revised version received 4 January 1996; accepted 8 January 1996)

Abstract

Micro-coiled ZrC fibres were prepared by the vapour phase metallizing of micro-coiled carbon fibres using a $ZrCl_4$ + H_2 + Ar gas mixture at 1100–1250°C. The preparation conditions, morphology and bulk electrical resistivity of the obtained ZrC coils were examined. The coiling morphology of the source coiled carbon fibres was fully preserved even after this treatment. The bulk resistivity of the coiled ZrC fibres decreased with bulk density and was 10^{-1} s^{-1} cm at 0·8 g cm^{-3}. © 1996 Elsevier Science Limited.

1 Introduction

Raw materials with a micro-coiled or helical morphology are not currently available. The helical morphology of DNA and some vine plants affords living bodies with essential functional roles. Accordingly, we could expect novel functional properties from such coiled materials. Addamiano[1] and Kang *et al.*[2] reported the preparation of micro-coiled SiC fibres using an impurity-activated chemical vapour deposition (CVD) process. Vogt *et al.*[3] prepared regularly micro-coiled Si_3N_4 fibres by the CVD process. We have obtained regularly micro-coiled Si_3N_4 fibres by the metal impurity-activated CVD process using Si_2Cl_6,[4–7] SiO_2 + C or SiO[8] as the Si source at 1200–1500°C. However, the growth of the micro-coiled fibres from the vapour phase was extremely accidental with low reproducibility. Johansson and Schweitz[9] prepared a boron spring by a laser-assisted CVD process using a three-dimensional micropositioning system. Macro-coiled ceramic springs or windings of above 5 mm in coil diameter were prepared by conventional calcination and sintering of an extruded polymer–ceramic suspension winding.[10] However, preparation of micro-coiled springs or fibres using these processes is very difficult.

We obtained regularly micro-coiled carbon fibres by the catalytic pyrolysis of acetylene with high coil yield and reproducibility.[11–15] Generally, carbon can easily be vapour phase metallized followed by solid-state diffusion to form the corresponding metal carbides. Accordingly, the metallization treatment of micro-coiled carbon fibres is considered to be the most promising process for obtaining micro-coiled fibres of the metal carbides. Coiled fibres of SiC[16] or TiC[14,15] were obtained by the CVD process or the metallizing of the coiled carbon fibres. However, their preparation conditions, morphology and characteristics have not been examined. The metal carbides have good properties such as high thermal and chemical stabilities, super-high hardness and high electrical conductivity. Thus their micro-coiled fibres are potential candidates for fillers in electromagnetic shielding materials, elastic packing or filter materials resistant to high temperatures and/or harsh or corrosive environments, and for micromechanical elements such as microsprings and micro sensors.

ZrC whiskers were prepared by the metal impurity-activated CVD process.[17–19] However, the deposition of coiled ZrC fibres has not been reported.

In this work, micro-coiled ZrC fibres were obtained by the vapour phase metallizing of the micro-coiled carbon fibres obtained by the catalytic pyrolysis of acetylene. The preparation conditions, morphology and electric resistivity of the coiled ZrC fibres were examined.

2 Experimental

Source micro-coiled carbon fibres (abbreviated as 'carbon coils' hereafter) were prepared by the Ni-metal catalysed pyrolysis of acetylene. The detailed preparation procedures and conditions

are given in Ref. 12. The used carbon coils are 1–5 μm in coil diameter and 50–500 μm in coil length. The source carbon coils were placed in a mullite boat which was located in the central part of a horizontal reaction tube (mullite, 20 mm i.d.). The carbon coils were vapour phase zirconized under a $ZrCl_4 + H_2 + Ar$ atmosphere at 1100–1250°C. The $ZrCl_4$ gas was prepared *in situ* by the chlorination of Zr sponge at 700°C and was carried by Ar into the reaction tube. Gas flow rates of $ZrCl_4$, H_2 and Ar were fixed at 5 sccm (ml s^{-1}), 100 sccm and 40 sccm, respectively.

3 Results and Discussion

3.1 Preparation of micro-coiled ZrC fibres

Figure 1 shows the influence of the square root of the zirconizing time on the zirconizing ratio of the source carbon coils as a function of reaction temperature. The zirconizing ratio was obtained from the weight gain due to zirconizing. The zirconizing ratio increased linearly with increasing zirconizing times irrespective of zirconizing temperature. Furthermore, it can be seen that the zirconizing ratio was only 25% after 4 h of zirconizing time at 1250°C. That is, the carbon coils were zirconized only near the surface under the conditions used in this work. The obtained zirconized carbon coils (abbreviated as 'ZrC coils' hereafter) have a carbon core which was not zirconized. The ZrC layers formed on the surface of the carbon coils were very dense without pores. The density of the formed ZrC layers was not examined. However, the above result suggests that the rate-determining step is diffusion of the Zr or carbon atoms through the formed ZrC layers.

The representative morphology of the ZrC coils obtained after zirconizing for 1 h at 1200°C is shown in Fig. 2. It was observed that the coiling morphology of the source carbon coils was fully preserved after zirconizing under any of the zirconizing conditions, except for a slight diameter increase in the carbon fibres. Carbon coils having a rectangular cross-section as well as those with the common circular cross-section as shown in Fig. 2 were sometimes observed in the source carbon coils. Flat or ribbon-like carbon coils were also zirconized with full preservation of the morphology to form flat or ribbon-like ZiC coils. Figure 3 shows various types of the flat or ribbon-like ZrC coils. Grain growth or secondary crystal growth on the surface of the ZrC coils was not observed even after zirconizing the carbon coils at 1250°C for 2 h, as shown in Fig. 4(b). The grain size of the ZrC observed on the surface was about 10 nm.

The X-ray diffraction (XRD) profiles of the ZrC coils obtained after a 60 min zirconizing time at 1100–1250°C are shown in Fig. 5. Apparent peaks indicating ZrC were not observed at 1100°C. Small peaks of $ZrCl_2$ as well as the apparent large peaks of ZrC were observed at 1200–1250°C. The $ZrCl_2$ decomposes above 350°C to form metal Zr and $ZrCl_4$. Accordingly, these peaks of $ZrCl_2$ may be caused by the contamination of the specimen by the $ZrCl_2$ by-product when the temperature was lowered. Figure 6 shows the XRD profiles of the ZrC coils obtained

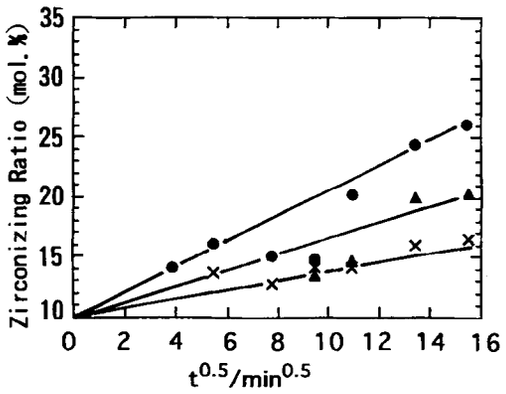

Fig. 1. Effect of square root of zirconizing time on the zirconizing ratio of the carbon coils. $ZrCl_4$ gas flow rate: 1·5 sccm, H_2 flow rate: 70 sccm, Ar flow rate: 40 sccm. Zirconizing temperature: ●, 1250°C, ▲, 1150°C, ×, 1100°C.

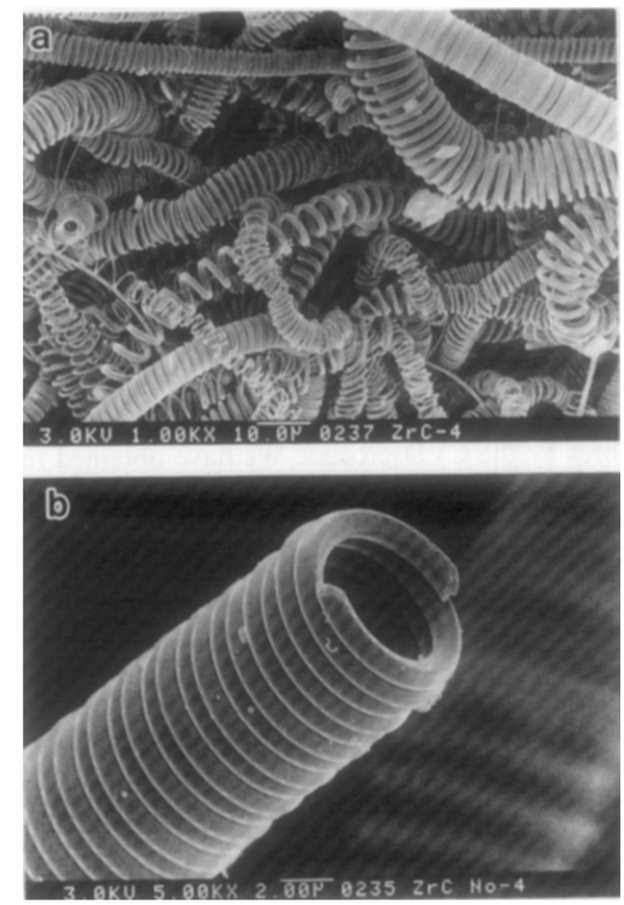

Fig. 2. Representative morphology of the ZrC coils (a) and the enlarged view (b).

after 15–120 min at 1250°C. Apparent peaks of ZrC were observed for a 15 min zirconizing time, and peaks were sharper with increasing zirconizing time.

Figure 7 shows a transmission electron micrograph (dark-field image) and electron diffraction profile. A halo ring (H) as well as Debye–Sherrer rings (A–D) are observed in Fig. 7(b). The source carbon coils used have an amorphous state, and this halo ring is caused by the unzirconized core part of the carbon coils. It is considered that the ZrC coils obtained in this work were only partly zirconized carbon coils, and the ZrC layers formed on the surface had a polycrystalline state.

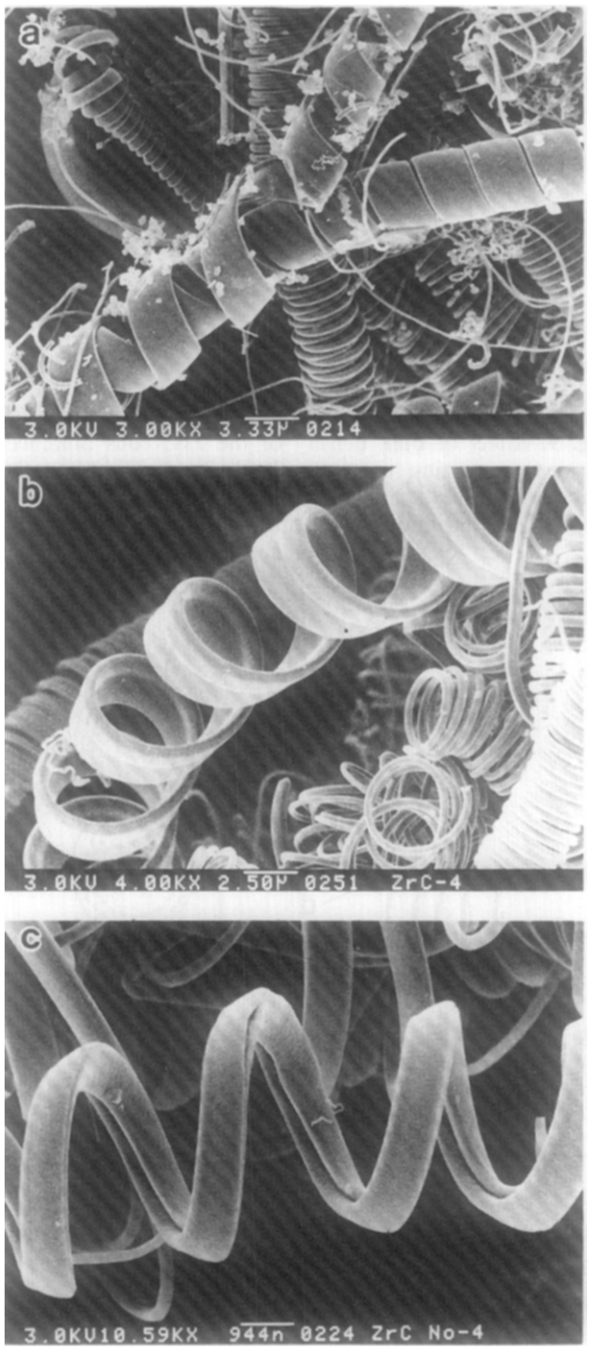

Fig. 3. Flat or ribbon-like ZrC coils. (a) Double ribbon-like coils, (b) single flat coil, (c) single coils having a deep ditch on the inside.

3.2 Bulk electrical resistivity of the ZrC coils

The bulk electrical resistivity of the ZrC coils was measured using a 10 mm i.d. cylindrical measurement cell. The effect of bulk density of the ZrC coils obtained at various zirconizing temperatures on the bulk electrical resistivity is shown in Fig. 8, in which zirconizing time was fixed for 120 min. The resistivity of the ZrC coils decreased

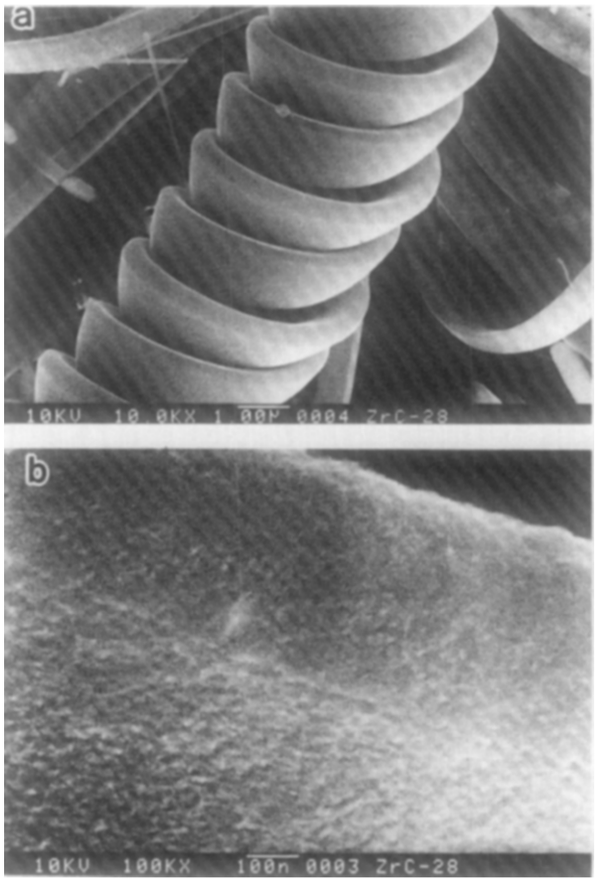

Fig. 4. ZrC coils having a rectangular cross-section (a) and the enlarged view (b).

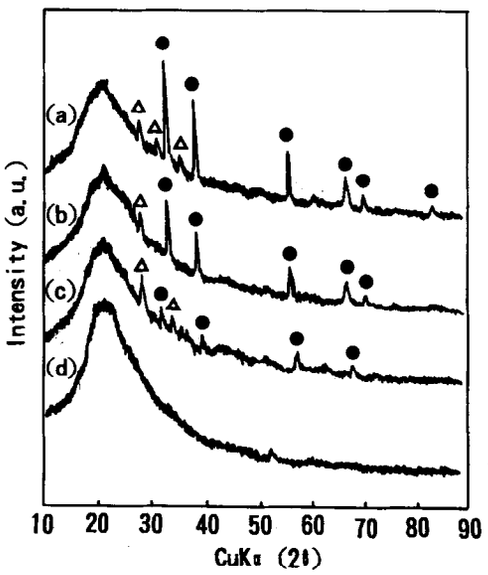

Fig. 5. XRD profiles of the ZrC coils obtained at various zirconizing temperatures. Zirconizing time: 60 min. Zirconizing temperature: (a) 1250°C, (b) 1200°C, (c) 1150°C, (d) 1100°C. ●, ZrC; Δ, $ZrCl_2$.

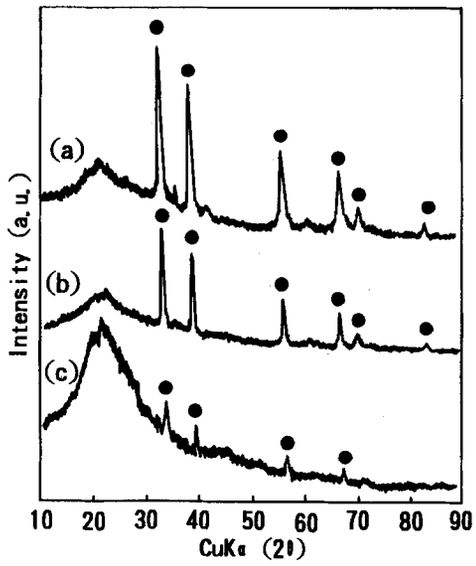

Fig. 6. XRD profiles of the ZrC coils obtained at various zirconizing times. Zirconizing temperature: 1250°C. Zirconizing time: (a) 180 min, (b) 120 min, (c) 15 min. ●, ZrC.

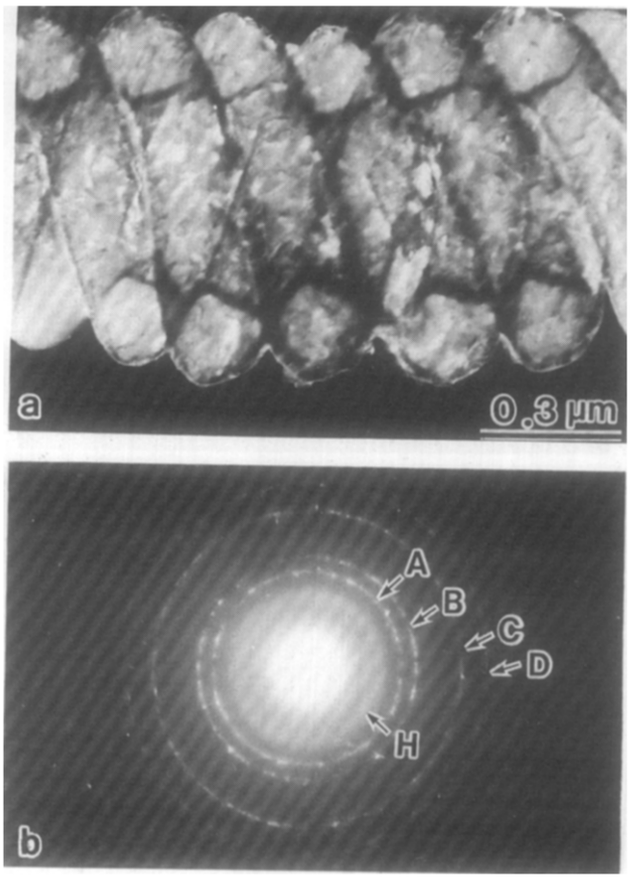

Fig. 7. Dark field image (a) and electron diffraction profile of the ZrC coils (b). A (111), B (200), C (220), D (311). H indicates halo pattern.

with increasing zirconizing time. No apparent effect of zirconizing temperature on the bulk resistivity was observed. The effect of zirconizing time on the bulk resistivity of ZrC coils is shown in Fig. 9, in which the zirconizing temperature was fixed at 1250°C. The bulk resistivity of the ZrC coils decreased with increasing zirconizing

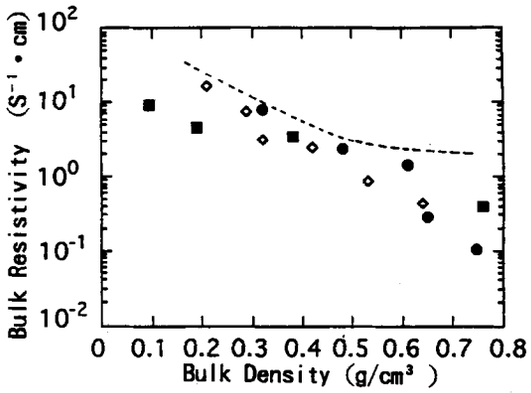

Fig. 8. Effect of bulk density of the ZrC coils obtained at various zirconizing temperatures on the bulk electrical resistivity. Zirconizing time: 180 min. Zirconizing temperature: ●, 1250°C; ■, 1200°C; ◊, 1150°C. ----, Source carbon coils.

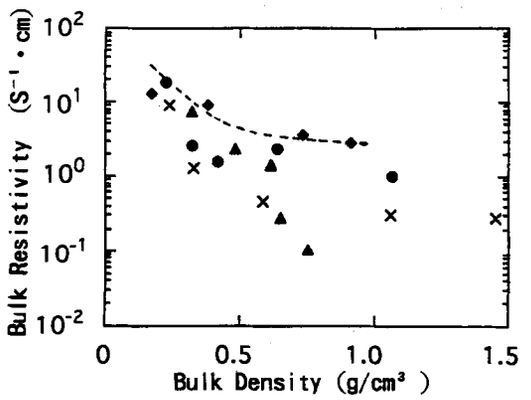

Fig. 9. Effect of bulk density of the ZrC coils obtained at various zirconizing times on the bulk electrical resistivity. Zirconizing temperature: 1250°C. Zirconizing time: ●, 15 min; ◆, 60 min; ×, 120 min; ▲, 180 min. ----, Source carbon coils.

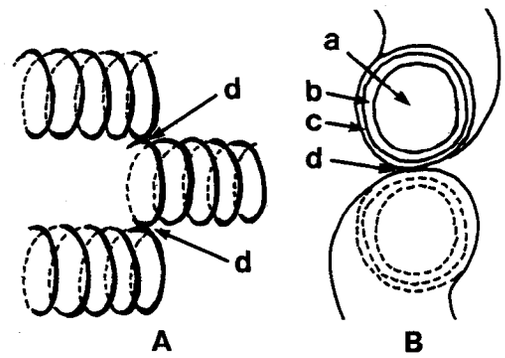

Fig. 10. Schematic contact conditions of the bulk ZrC coils (A) and the enlarged cross-section (B). a, Carbon core; b, ZrC clad; c, Zr-oxide layers; d, contact part.

time and attained a low value of about 10^{-1} s^{-1} cm at 0·8 g cm^{-3} for 120 min zirconizing time. The electric contact conditions in the bulk ZrC coils and the cross-section of the contact part are shown schematically in Fig. 10. It is postulated that very thin zirconium oxide layers are formed on the surface of the ZrC layers (ZrC clads). Accordingly, the bulk electrical resistivity of the ZrC coils, R, can be estimated by the equations

$$\frac{1}{R_b} = \frac{1}{R_c} + \frac{1}{R_z} + \frac{1}{R_o} \quad (1)$$

$$R = R_b + R_a + R_c \quad (2)$$

where R_b, R_c, R_z and R_o are the electrical resistivity of the ZrC coils, source carbon coils (carbon core), ZrC layers (ZrC clad) and zirconium oxide layers formed on the ZrC clad, respectively, and R_a is a contact resistivity between the ZrC coils. The density and electrical resistivity of the ZrC clad as well as the carbon core are not known. The densities of the $ZrC_{1.0}$ single crystal and amorphous carbon is 4·0 g cm^{-3} and about 2·0 g cm^{-3}, respectively. The carbon coils are in an amorphous state. The ZrC coils obtained at 1250°C for 120 min have a ZrC clad with 20% of the total cross-section, and the density of the ZrC coils is estimated to be 2·4 g cm^{-3}. The electrical resistivities of the $ZrC_{0.97}$ crystal and vapour-grown straight carbon fibres are 5×10^{-4} s^{-1} cm (Ref. 20) and 1×10^{-3} s^{-1} cm (Ref. 21), respectively.Accordingly, the electrical resistivity of the ZrC coils is estimated to be $3{\cdot}6 \times 10^{-4}$ s^{-1} cm. This value is two orders of magnitude lower than that of 1×10^{-1} s^{-1} cm obtained for the bulk ZrC coils with a bulk density 0·8 g cm^{-3}, as can be seen in Fig. 8. The bulk ZrC coils with a bulk density of 0·8 g cm^{-3} are more expanded (by about three times) than the ZrC coils with a density of 2·4 g cm^{-3}. Therefore, the area of the contact point between each ZrC coil, through which electric current is conducted, may be smaller than that for the cross-section of a ZrC coil, which may result in an increased electrical resistivity. Furthermore, zirconium oxide layers formed on the surface of the ZrC clads may act as a large barrier for electrical conduction. That is, the observed electrical resistivity of the bulk ZrC coils is larger than that estimated theoretically because of the small contact area between each ZrC coil and the presence of oxide layers.

4 Conclusions

Micro-coiled ZrC fibres were prepared by vapour phase zirconizing of micro-coiled carbon fibres, and their preparation conditions, morphology and bulk electrical resistivity were examined. The coiling morphology of the source carbon coils was fully preserved under all zirconizing conditions. The bulk resistivity of the coiled ZrC fibres decreased with bulk density and was 10^{-1} s^{-1} cm at 0·8 g cm^{-3}.

Acknowledgements

This work was supported by the Kawasaki Steel 21st Century Foundation, Iketani Science and Technology Foundation, Murata Science Foundation and Yazaki Memorial Foundation for Science and Technology.

References

1. Addamiano, A., *J. Cryst. Growth*, **58** (1982) 617–22.
2. Kang, T.-K., Park, S.-D., Rhee, C.-K. & Kuk, Il-H., *Proc. 6th Japan–Korea Ceramic Seminar* (1989, Kobe), pp. 249–53.
3. Vogt, U., Hofmann, H. & Kramer, V., *Key Eng. Mater.*, 89–91 (1994) 29–34.
4. Motojima, S., Ueno, S., Hattori, T. & Goto, K., *Appl. Phys. Lett.*, **54** (1989) 1001–3.
5. Motojima, S., Ueno, S., Hattori, T. & Iwanaga, H., *J. Cryst. Growth*, **96** (1989) 383–9.
6. Iwanaga, H., Kawaguchi, M. & Motojima, S., *Jpn J. Appl. Phys.*, **32** (1993) 105–15.
7. Iwanaga, H., Iwasaki, T., Motojima, S. & Takeuchi, S., *J. Mater. Sci. Lett.*, **9** (1990) 731–4.
8. Motojima, S., Yamana, T., Araki, T. & Iwanaga, H., *J. Electrochem. Soc.*, **142** (1995) 3141–8.
9. Johannson, S. & Schweitz, J.-A., *J. Appl. Phys.*, **72** (1992) 5956–63.
10. Wright, J. K., Thomson, R. M. & Evance, J. R. G., *J. Mater. Sci.*, **25** (1990) 149–56.
11. Motojima, S., Kawaguchi, M., Nozaki, K. & Iwanaga, H., *Appl. Phys. Lett.*, **56** (1990) 321–3.
12. Motojima, S., Kawaguchi, M., Nozaki, K. & Iwanaga, H., *Carbon*, **29** (1991) 379–85.
13. Motojima, S., Hasegawa, I., Kagiya, S., Momiyama, M., Kawaguchi, M. & Iwanaga, H., *Appl. Phys. Lett.*, **62** (1993) 2322–3.
14. Motojima, S., Kawaguchi, M., Nozaki, K. & Iwanaga, H., *Proc. 11th Int. Conf. CVD* (1990, Seattle), pp. 573–9.
15. Motojima, S., Hasegawa, I., Kawaguchi, M., Nozaki, K. & Iwanaga, H., *J. Chem. Vapor Deposition*, **1** (1992) 136–56.
16. Unpublished data.
17. Naito, K., Kamegashira, N. & Fujiwara, N., *J. Cryst. Growth*, **45** (1978) 506–10.
18. Tamari, N. & Kato, A., *Nippon Kagaku Kaishi, J. Chem. Soc. Jpn*, (1977) 650–5.
19. Tamari, T. & Kato, A., *J. Less-Common Met.*, **58** (1978) 147–60.
20. Endo, M., *Chemtech*, (1988) 568–76.
21. In *Tugoplakie Soedineniya*, eds G. V. Samsonov & I. M. Vinitskii. Moskva, 1976.